Journal of Solid State Chemistry 183 (2010) 1891–1899

Contents lists available at ScienceDirect

Journal of Solid State Chemistry

journal homepage: www.elsevier.com/locate/jssc

Processing and characterization of new oxy-sulfo-telluride glasses in the Ge–Sb–Te–S–O system

C. Smith [a], J. Jackson [a], L. Petit [a,*], C. Rivero-Baleine [b], K. Richardson [a]

[a] School of Materials Science and Engineering, Clemson University, Clemson, SC 29634, USA
[b] Lockheed Martin Missiles and Fire Control, Orlando, FL 32819, USA

ARTICLE INFO

Article history:
Received 9 March 2010
Received in revised form
25 May 2010
Accepted 14 June 2010
Available online 19 June 2010

Keywords:
Chalcogenide
Oxy-sulfo-telluride glass
Raman spectroscopy

ABSTRACT

New oxy-sulfo-telluride glasses have been prepared in the Ge–Sb–Te–S–O system employing a two-step melting process which involves the processing of a chalcogenide glass (ChG) and subsequent melting with TeO_2 or Sb_2O_3. The progressive incorporation of O at the expense of S was found to increase the density and the glass transition temperature and to decrease the molar volume of the investigated oxy-sulfo-telluride glasses. We also observed a shift of the vis–NIR cut-off wavelength to longer wavelength probably due to changes in Sb coordination within the glass matrix and overall matrix polarizability. Using Raman spectroscopy, correlations have been shown between the formation of Ge- and Sb-based oxysulfide structural units and the S/O ratio. Lastly, two glasses with similar composition ($Ge_{20}Sb_6S_{64}Te_3O_7$) processed by melting the $Ge_{23}Sb_7S_{70}$ glass with TeO_2 or the $Ge_{23}Sb_2S_{72}Te_4$ glass with Sb_2O_3 were found to have slightly different physical, thermal, optical and structural properties. These changes are thought to result mainly from the higher moisture content and sensitivity of the TeO_2 starting materials as compared to that of the Sb_2O_3.

1. Introduction

There is growing interest in families of specialty glasses incorporating fluorine, chalcogenide (ChG) and heavy metal oxide (HMO) components. Such glasses are attractive due to their mid-infrared (MIR) and (for non-oxides) long wave infrared (LWIR) transparency, low phonon energies and high refractive indices as compared to SiO_2 [1,2]. Chalcogenide glasses (ChGs) have been studied extensively over the past 50 years and have grown in use despite their limited thermal and mechanical stability. These limitations can be attributed to weaker bond strengths between the constituent atoms that result in lower glass transition temperatures; the lower T_g comes with the trade-off of good IR transmission that results from the glasses' large constituent ions and molar mass [3]. ChGs continue to see expanded use in infrared telecommunication applications and integrated optics [4–6] as these glasses are known to possess adequate chemical and mechanical durability for these applications and possess wide glass-forming regions and extended infrared transparency versus HMOs. For example, the As_2S_3 glass transmits up to 12 μm [7], while additions of halide can reach wavelengths near 20 μm. These glasses (can) exhibit large linear and non-linear optical properties, which influence their use in high power applications, and without purification, multicomponent ChGs can exhibit large intrinsic MIR losses due to hydride and oxide impurities [8,9]. Additionally, ChGs can be mechanically soft and sensitive to band gap light exposure which can often limit their applications [10,11].

For the past five years, we have studied the processing and characterization of new Ge-based chalcogenide glasses [12–15]. In order to enhance the mechanical properties of these new glasses and reduce their chalcogen-induced photo-sensitivity, we have investigated the impact of partial replacement of sulfur atoms in the ChG network by oxygen atoms. The motivation for such replacement is to selectively incorporate the robust mechanical properties of oxide materials with the attractive optical traits of sulfide glasses, by adjusting the chalcogen to oxygen ratio. The early work by Zhou et al. [16] suggested that oxysulfide glasses possess good chemical durability combined with high optical nonlinearity as compared to pure sulfides, indicating that the partial incorporation of oxygen-containing bonds can enhance the overall bond strength of the mixed (group VI-containing) oxysulfide glasses.

A key challenge in the effective preparation and use of chalcogenide and oxy-chalcogenide glasses is the reliance on preparation routes requiring heat treatments in closed systems. Such closed systems are necessary to contain the high vapor pressure produced by constituents such as sulfur, during the melting. Kim et al. [17] showed that germanium oxysulfide glasses, with the compositions $(1-x)GeS_2-xGeO_2$ for $0<x<1$,

* Corresponding author.
E-mail address: lpetit@clemson.edu (L. Petit).

0022-4596/$ - see front matter © 2010 Elsevier Inc. All rights reserved.
doi:10.1016/j.jssc.2010.06.009

can be prepared by rapidly quenching melts sealed in silica tubes to room temperature. However, these oxysulfide glasses are thought to be heterogeneous over a nano-scale due to phase separation phenomenon [18].

We previously demonstrated that a sulfination heat treatment of GeO_2 powder can lead to the formation of germanium oxysulfide powder, which can be formed into a target and deposited into amorphous GeS_2–GeO_2 films using an RF sputtering technique [13]. We have also investigated an alternative technique to process oxysulfide glasses using a two-step process which involves the melting of a chalcogenide glass with an oxide powder [14]. We showed that the melt of a sulfide-based glass with GeO_2 or Sb_2O_3 can lead to the formation of an oxysulfide glass with controlled S/O ratio where both O and S are fully integrated in the glass network. More recently, we successfully demonstrated the processing of active oxysulfide glasses through the melting of a chalcogenide glass with Er_2O_3 and Sb_2O_3 and also by melting an Er^{3+} doped chalcogenide glass with Sb_2O_3 [15]. This resulted in active glasses with the same composition, processed using different chalcogenide matrix/oxide powder systems, which exhibited slightly different emission spectra due to slightly different local rare earth environment associated with the chalcogenide matrix/oxide powder systems.

Following on this result, we have expanded this investigation towards the processing of new oxy-chalcogenide glasses through the melting of various chalcogenide matrix/oxide powder systems to verify the impact of the starting materials on the physical, thermal, optical and structural properties of the resulting oxy-chalcogenide glass. This paper discusses our most recent findings on the processing and characterization of new ChG glasses prepared with small levels of Te, melted either with TeO_2 or Sb_2O_3 powders. These new glasses have been labeled oxy-sulfo-telluride glasses. First, we present the processing of these new germanium-based oxy-sulfo-telluride glasses prepared from the melting of (a) a $Ge_{23}Sb_7S_{70}$ glass with TeO_2 and (b) a $Ge_{23}Sb_7S_{65}Te_5$ glass with Sb_2O_3. The structural changes induced by the addition of oxygen have been systematically investigated as a function of O/S ratio using Raman spectroscopy and have been correlated to the physical, thermal and optical properties of the investigated glass. Lastly, we compare the properties listed above for two oxy-sulfo-telluride glasses processed with similar composition ($Ge_{20}Sb_6S_{64}Te_3O_7$) by melting the $Ge_{23}Sb_7S_{70}$ glass with TeO_2 or the $Ge_{23}Sb_2S_{72}Te_4$ glass with Sb_2O_3 to ascertain the role of the glass starting materials on the resulting material properties.

2. Experimental

Bulk germanium oxy-sulfo-telluride glasses were prepared with different O/S ratios using a two-step melting process in order to determine the maximum concentration of oxygen that can be incorporated without crystallization or phase separation. The first step consisted of the processing of the sulfo-telluride glass which was subsequently melted with Sb_2O_3 or TeO_2 powder.

Chalcogenide bulk glasses in the system Ge–Sb–S–Te were prepared in 15 g batches using high purity elements (Ge and Te: Alfa Aesar 99.999% and Sb and S: Sigma Aldrich 99.998%). Starting materials were weighed and batched into quartz ampoules inside a nitrogen-purged glove box and sealed under vacuum using a methane–oxygen torch. Prior to sealing and melting, the ampoule and batch were pre-heated at 100 °C for 4 h to remove potential surface moisture from the quartz ampoule and the batch raw materials. The ampoule was then sealed and heated for 24 h at 900–925 °C, depending on the glass composition. A rocking furnace was used to rock the ampoule to increase the homogeneity of the melt. Once homogenized, the melt-containing ampoule was air-quenched to room temperature. To avoid fracture of the tube and glass ingot, the ampoules were subsequently returned to the furnace for annealing for 15 h at 40 °C below the glass transition temperature (T_g) of the investigated glasses.

The oxy-sulfo-telluride glasses with compositions (a) $(1-x)Ge_{23}Sb_7S_{70}-xTe_{33}O_{67}$ with $x=0$, 0.038, 0.10 and 0.15 and (b) $(1-y)Ge_{23}Sb_2S_{72}Te_4-ySb_{40}O_{60}$ with $y=0$, 0.085, 0.15 and 0.2, were prepared by melting in vacuum 3 g of the ChG glass with TeO_2 (Alfa Aesar, 99%) or Sb_2O_3 (Aldrich, 99%) in covered graphite crucibles within a quartz ampoule. The graphite crucible was used as a barrier between the melt and the ampoule to prevent a reaction between the silica tube and the oxide powder and the typical sticking to quartz that is observed for oxide-containing glasses. Note that for the calculation of the resulting oxy-sulfo-telluride atomic concentration, TeO_2 is expressed in molar fraction as $Te_{33}O_{67}$ and Sb_2O_3 as $Sb_{40}O_{60}$.

Prior to melting, the ampoule was sealed under vacuum. The melting temperature of 925 °C was reached with a 2.5 °C/min heating ramp without rocking the furnace due to containment of the melt within the graphite crucible. After melting, the glass was quenched in air and the oxy-sulfo-telluride glasses were removed from the graphite crucible and annealed in air at 40 °C below the glass transition temperature of the glass for 15 h. The oxy-sulfo-telluride glasses (OChGs) were stored in a dry nitrogen environment within a glove box prior to use. The ChG and OChG samples were then cut, optically polished and inspected visually.

The polished sulfo-telluride and oxy-sulfo-telluride glasses were analyzed for composition using an energy-dispersive spectroscopy (EDS) system coupled to a scanning electron microscope (SEM). Some carbon particulate contamination was observed in the resulting glass specimens via SEM (and confirmed with EDS). This particulate is undoubtedly from the melt's contact with the graphite crucible.

The glass transition temperature (T_g) was measured using a model 2940 differential scanning calorimeter (DSC) from TA Instruments (TA Instruments Corp. http://www.tainstruments.com) at a heating rate of 10 °C/min over a temperature range of 40–450 °C. The measurements were carried out in a hermetically sealed aluminum pan. The glass transition temperature was taken at the inflection point of the endotherm, as obtained by taking the first derivative of the DSC curve. T_g was determined with an accuracy of ± 2 °C.

The density of the glasses was measured by the Archimedes' principle using diethyl phthalate as the immersion liquid, with an accuracy of ± 0.02 g/cm^3. The molar volume of the glasses was determined by dividing the molecular weight of the glass by its density.

The visible–near infrared (vis–NIR) and infrared absorption spectra were measured at room temperature using a Perkin Elmer Lambda 900 UV/vis/NIR spectrometer and a Magna-IR 560 spectrometer from Nicolet, respectively. For all measurements, the samples were optically polished to a thickness of 1–3 mm.

The structural analysis of the glasses was carried out using Raman spectroscopy on a LabRam HR system. This system has a typical resolution of about 1 cm^{-1} at room temperature and uses a backscattering geometry. The system consists of a holographic notch filter for Rayleigh rejection, a confocal microscope equipped with a 100× objective and a CCD detector. A 785 nm NIR semiconductor laser was used for excitation with an incident power of around 10 mW. Since our excitation wavelength falls in the absorption region for some of the compositions studied here, the laser power was adjusted so that no photo-structural damage was induced in the glass during the Raman measurements.

3. Results and discussion

The aim of this study was to investigate the processing and characterization of new germanium-based oxy-sulfo-telluride glasses which have been prepared by melting ChG glasses with TeO_2 or Sb_2O_3 powders. Raman spectroscopy has been employed to track and evaluate structural modifications caused by the systematic replacement of S by O through the use of various starting materials. We interpret the evolution of Raman spectral features, which are indicative of local bonding in the glass network, to understand the correlations between the glass' structural characteristics and the corresponding physical, thermal and optical properties of such glasses. Finally, we compare the specific properties of two oxy-sulfo-telluride glasses with similar composition processed using two different ChG matrix/oxide powder systems.

3.1. Processing and characterization of oxy-sulfo-telluride glasses using TeO_2

Oxysulfide glasses have been obtained by incorporating TeO_2 in the $Ge_{23}Sb_7S_{70}$ glass network. No apparent crystallization or phase separation was observed in the glasses with the incorporation of TeO_2 up to $x=0.15$ as determined via visual inspection of the glasses. Table 1 gives the nominal glass compositions and those obtained from the EDS analysis (neglecting the small level of carbon contamination from the graphite crucible), the density, the molar volume and the glass transition temperature of the investigated glasses. The introduction of TeO_2 in the sulfide network leads to an increase of the density and a decrease of the glass transition temperature, T_g. These variations are due, not only to the partial replacement of sulfur by oxygen but also to the incorporation of the Te content.

In order to separate the contribution of the S/O ratio change from that of the Te addition, glasses have been prepared such that the ratio between the cations for the sulfo-telluride glasses is the same as the ratio between the cations for the oxy-sulfo-telluride glasses. The physical and thermal properties of these glasses are also listed in Table 1. One can notice that the density of the sulfo-telluride glasses increases and T_g decreases as the Te content increases up to 5 at% at the expense of the Ge content which decreases from 23 to 20 at%. These variations in the physical and thermal properties of the glass can be mainly related to the atomic radius of Ge which is smaller than that of Te. Changing the composition by increasing the Te content at the expense of the Ge content results in an increase of the glass density and in the formation of weaker bonds than those formed with S, thus decreasing the T_g. The small decrease of the molar volume with the incorporation of 1 at% of Te can be related to the decrease of the Ge content from 23 to 21 at% which (slightly) decreases the extent of cross-linking of the structure. This change would also lead to a reduction in the molar volume as suggested by [19]. However, as the concentration of Te increases from 1 to 5 at%, the molar volume of the glass increases due to the much larger mass and atomic radius of the Te atoms compared to the Ge atoms in agreement with [20].

The influence of chalcogen substitution is also illustrated in the physical property data in Table 1. When sulfur is replaced by oxygen, the density and T_g increase and the molar volume decreases. These variations in the physical and thermal properties with the progressive incorporation of oxygen, which has a smaller mass and atomic radius than S, can be related to a change of the network organization. Oxygen is expected to form stronger glass network bonds leading to an increase of the T_g, while its smaller ionic radius would contribute to the observed decrease in the molar volume.

The absorption spectra of the oxy-sulfo-telluride glasses are shown in Fig. 1a. The absorption edge shifts to larger wavelengths when TeO_2 is introduced in the $Ge_{23}Sb_7S_{70}$ network. Shown in Fig. 1b are the absorption spectra of the sulfo-telluride and oxy-sulfo-telluride glasses with similar cation ratios. Clearly, the spectra show that Te is not the only contributor to the red shift of the absorption band gap but also the replacement of S by O plays a role. The red shift induced by the replacement of S by O is in disagreement with our previous studies [13–15] and is believed to be related to a change in the coordination number of some of the Sb cations when oxygen is introduced in the glass network [21]. The transmission spectra of some of the ChG and OChG glasses are depicted in Fig. 1c. One can notice that the introduction of Te in the sulfide network increases the long wave cut off to longer wavelength whereas the replacement of sulfur by oxygen decreases it. As the samples do not have the same absorption (which is a function of the glass thickness), it is not possible to compare the transmission % of the glass as a function of the replacement of sulfur by Te or O. However, we expect the transmission of the Te-containing glasses to be lower than that of S-containing glasses and even lower than that of O-containing glasses in agreement with [22]. Several absorption bands associated with impurities in the glass matrix can also be seen in the spectra for these glasses where no special effort at raw material purification prior to the melting has been made.

In order to compare the level of impurities, the infrared absorption spectra of the glasses were measured. The spectra of the oxy-sulfo-telluride glasses are shown in Fig. 2. The spectra exhibit weak bands near the 1270–1315 cm^{-1} range and at 1500, 2000, 2330, 2500, 3246, 3500 and 3737 cm^{-1}. In agreement with [23], the bands near the 1270–1315 cm^{-1} range can be related to S–O groups, the band near 3246 cm^{-1} corresponds to the stretch modes of OH hydroxyl groups and the band near the 3737 cm^{-1} to the vibrational bands of the hydroxyl containing groups and

Table 1
Nominal and analyzed composition, density, molar volume and glass transition temperature (T_g) of the investigated sulfo-telluride and oxy-sulfo-telluride glasses in the system $(1-x)Ge_{23}Sb_7S_{70}+xTe_{33}O_{67}$.

Glass (Batch composition)	Composition measured by EDS ($\pm 2\%$)	Density (g/cm^3) ± 0.02 g/cm^3	Molar volume (cm^3/mol) ± 0.09 cm^3/mol	T_g (°C) ± 2 °C
$(1-x)Ge_{23}Sb_7S_{70}-xTe_{33}O_{67}$				
$x=0$ $Ge_{23}Sb_7S_{70}$	$Ge_{23}Sb_7S_{70}$	2.94	16.21	311
$x=0.038$ $Ge_{21}Sb_7S_{68}Te_1O_3$	$Ge_{22}Sb_6S_{53}Te_1O_5$	3.04	15.57	316
$x=0.10$ $Ge_{20}Sb_6S_{63}Te_3O_7$	$Ge_{21}Sb_7S_{59}Te_4O_9$	3.15	14.91	304
$x=0.15$ $Ge_{20}Sb_6S_{59}Te_5O_{10}$	$Ge_{20}Sb_6S_{57}Te_5O_{11}$	3.19	15.27	289
Corresponding sulfo-telluride glasses				
$Ge_{21}Sb_7S_{71}Te_1$		3.03	15.78	304
$Ge_{20}Sb_6S_{69}Te_5$		3.10	16.23	253

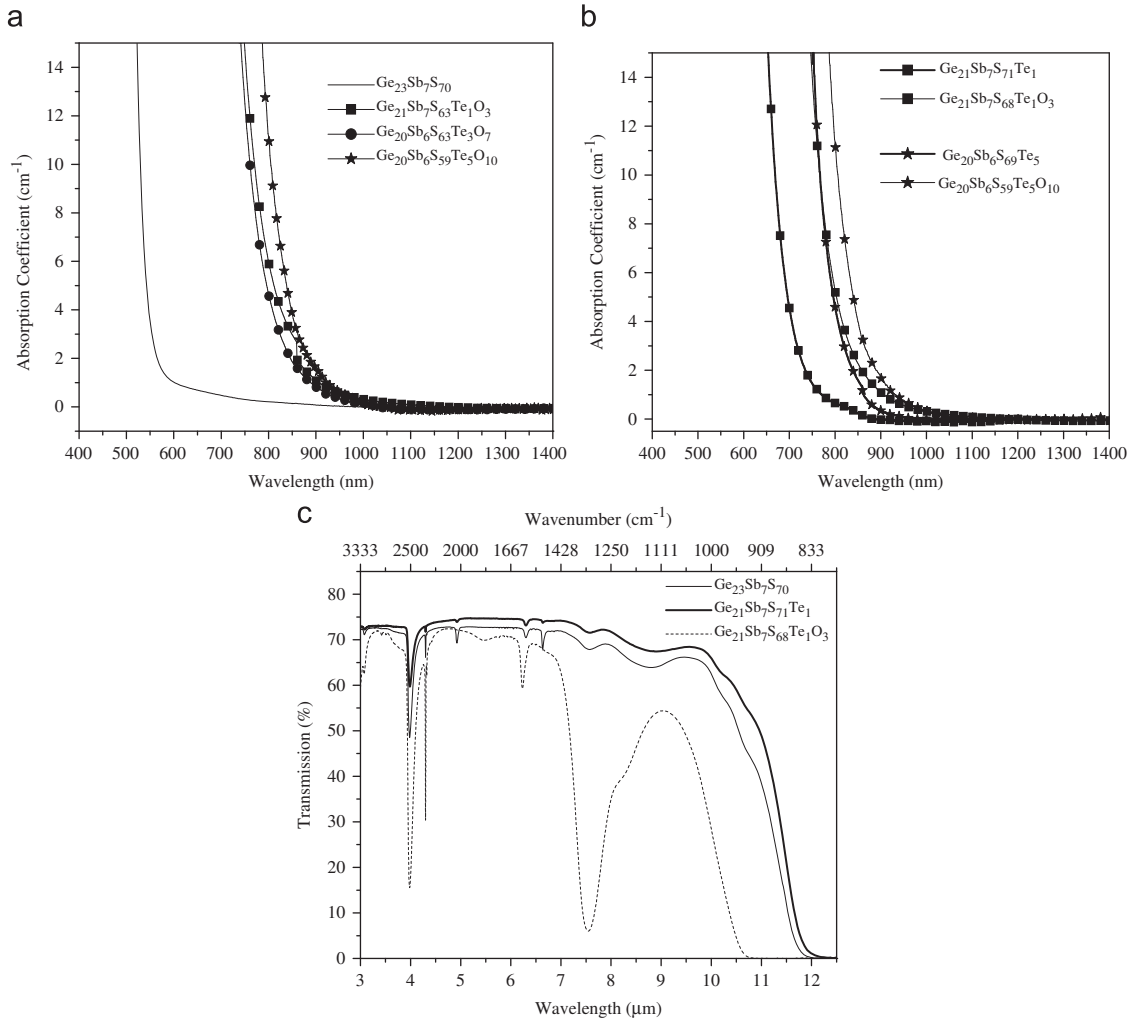

Fig. 1. Absorption spectra of the OChG glasses in the system $(1-x)Ge_{23}Sb_7S_{70}+xTe_{33}O_{67}$ (a) and of the ChG and OChG with the same ratio between the cations (b) and transmission spectra of some ChG and OChG glasses in the system $(1-x)Ge_{23}Sb_7S_{70}+xTe_{33}O_{67}$.

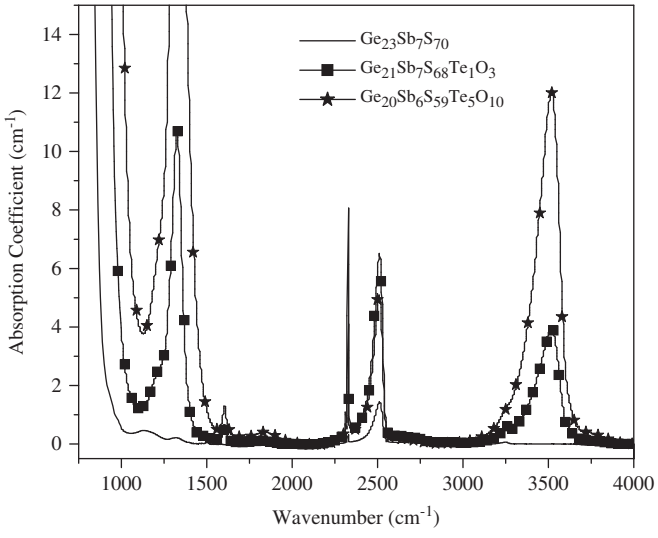

Fig. 2. IR absorption spectra of the OChG in the system $(1-x)Ge_{23}Sb_7S_{70}+xTe_{33}O_{67}$.

molecular water. The band near 1500 and 3500 cm^{-1} correspond to H_2O molecular-adsorbed IR vibrational bands, and the bands at 2330 and 2500 cm^{-1} are attributed to molecular H_2S and S–H complexes, respectively. The band at ~2000 cm^{-1} can be related to C–O–S carbon containing groups [23]. When oxygen is introduced in the glass network by adding TeO_2, the amplitude of all the bands at 1295, 1320, 1500, 2330, 2500, 3246, 3500 and 3737 cm^{-1}increases dramatically indicating an increase of the S–O, H_2S, S–H, OH impurities content, respectively. It is interesting to point out that the absorption edge shifts to larger wavenumber when sulfur is replaced by oxygen, confirming the incorporation of oxygen into the sulfo-telluride network.

The normalized Raman spectra of the investigated sulfo-telluride and oxy-sulfo-telluride glasses are presented in Fig. 3a, b and c. The spectra exhibit a broad feature with a maximum near 340 cm^{-1}, which is formed by the overlap of multiple Raman vibrations and smaller bands near 475 cm^{-1} as explained in [24]. The shoulder near 300 cm^{-1} has been assigned to the E modes of $SbS_{3/2}$ pyramids. In agreement with [25–28], the bands at 330 and the shoulder at 400 cm^{-1} have been assigned to the A_1 and T_2 modes of corner sharing $GeS_{4/2}$ groups with a smaller contribution of the E mode of the $SbS_{3/2}$ pyramids. The shoulders at 340, 375 and 420 cm^{-1} have been attributed, respectively, to A_1 mode of the GeS_4 molecular units, to the T_2 mode of edge-sharing $Ge_2S_4S_{2/2}$ tetrahedra and to the vibration of two tetrahedra connected through a bridging sulfur $S_3Ge–S–GeS_3$. At higher wavenumbers, the band at ~475 cm^{-1} can be attributed to the S_8 (A_1) ring vibration mode and at 485 cm^{-1} to vibration mode of S (A_1) chain [28].

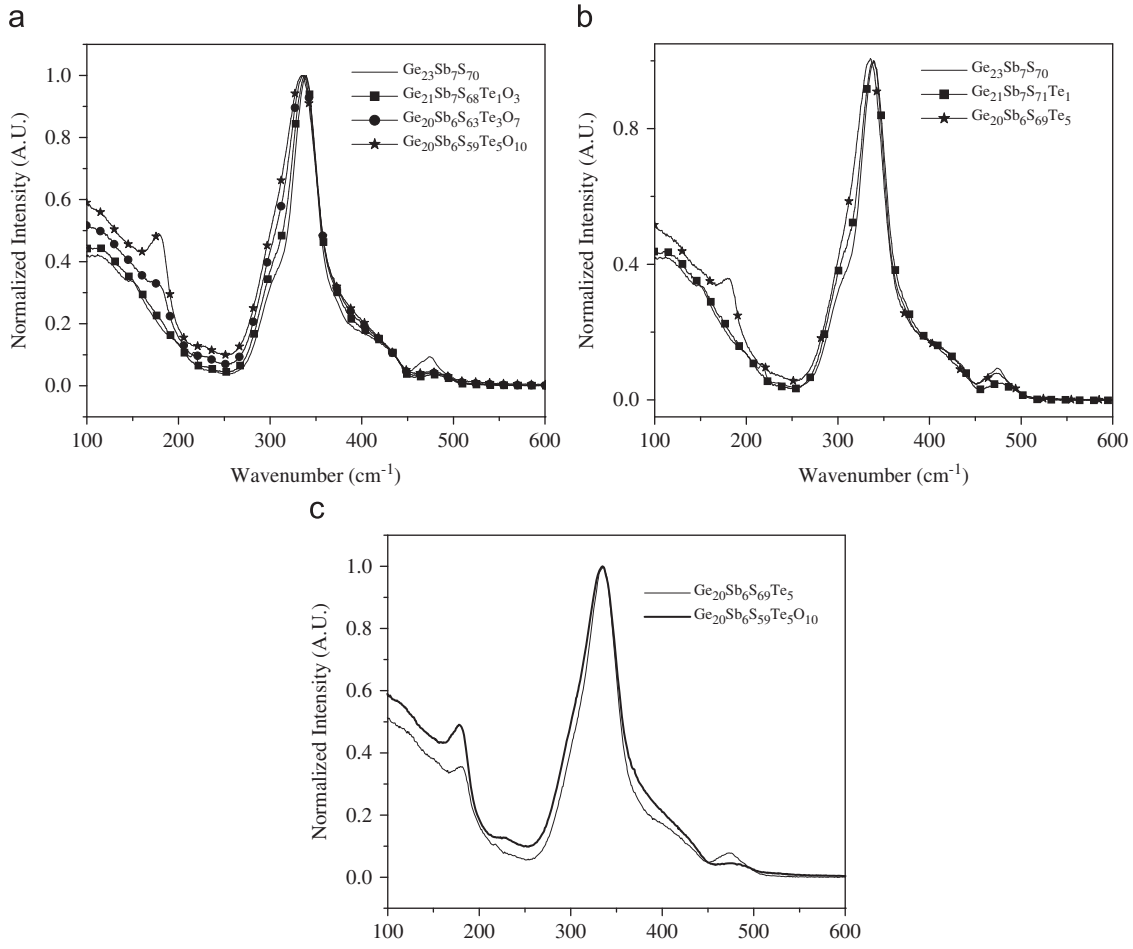

Fig. 3. Raman spectra of the OChG glasses in the system $(1-x)Ge_{23}Sb_7S_{70}+xTe_{33}O_{67}$ (a), of the sulfo-telluride glasses (b) and of the ChG and OChG with the same ratio between the cations (c).

When TeO_2 or Te is introduced into the sulfo-telluride glass network (Fig. 3a and b), the amplitude of the band at 475 cm^{-1} decreases compared to that of the main band, revealing a decrease of the S–S homopolar bonds in agreement with the decrease of the S content. Also, a new band at ~180 cm^{-1} develops, which, in agreement with [29–31], can be related to the formation of Ge–Te in edge-sharing $GeTe_4$ tetrahedra and Sb–Te bonds in Sb_2Te_3 units. One can notice in Fig. 3b that the main band shifts to higher wavelength when Te is added in the network. In agreement with [13,14], this might indicate the changes in the interconnectivity of the GeS_4 tetrahedra associated with a decrease of the $GeS_{4/2}$ units in the glass network. This is probably due to variations in the sulfur content and to the formation of new Ge–Te bonds confirming the incorporation of Te in the glass network.

In order to understand the real effect of S replacement by O without the contribution of the Te content increase, the Raman spectra of the ChG and OChG glasses with the same ratio between the cations are compared in Fig. 3c. The replacement of sulfur by oxygen leads to an increase of the shoulder in the 350–450 cm^{-1} range and at ~300 cm^{-1}, a decrease of the band at 475 cm^{-1}, and also a small shift to lower wavenumber of the band at ~180 cm^{-1}. A small (but significant) shift of the main band to lower wavenumber was also observed. The main band was fitted as performed elsewhere [13–15] but could not be obtained by simple summation of GeS_2 vibrational features to the oxide spectra. The addition of a new band between 360 and 400 cm^{-1}, different from GeO_4 or GeS_4 tetrahedral sites, was necessary to correctly simulate the spectrum. We observed that the intensity of this band increases with an increase of O content. In agreement with [13,14], this band can be attributed to the presence of edge-sharing $GeS_{4/2}$ tetrahedra (shoulder at ca. 375 cm^{-1}) which in the presence of oxygen, can transform to form mixed oxysulfide tetrahedral units such as GeO_3S, GeO_2S_2 or $GeOS_3$.

In summary, the analysis of the IR and Raman spectra clearly shows that introduction of TeO_2 in the Ge–Sb–S glass induces (i) changes in the interconnectivity of GeS_4 tetrahedra due to variations in the sulfur content, (ii) formation of new Ge–Te and Sb–Te bonds and (iii) formation of new oxysulfide units such as $GeOS_3$, GeO_2S_2 or GeO_3S. These structural changes are consistent with the increase of the density and T_g and also with the decrease of the molar volume (Table 1) in the glasses.

3.2. Processing and characterization of oxy-sulfo-telluride glasses using Sb_2O_3

We have previously demonstrated the successful processing of OChG using Sb_2O_3 powder [14,15]. In order to prepare new oxy-sulfo-telluride glasses using Sb_2O_3, the glass with the composition $Ge_{23}Sb_7S_{65}Te_5$ was re-melted with varying levels of Sb_2O_3. No phase separation or crystallization was observed in the oxy-sulfo-telluride glasses with the incorporation of Sb_2O_3 up to $y=0.2$ as determined via visual inspection of the glasses. Table 2 illustrates the nominal glass compositions and those obtained from the EDS analysis (without considering carbon contamination from the graphite crucible), the density, T_g and molar volume of the new

Table 2
Nominal and analyzed composition, density, molar volume and glass transition temperature (T_g) of the investigated sulfo-telluride and oxy-sulfo-telluride glasses in the system $(1-y)Ge_{23}Sb_7S_{65}Te_5+ySb_{40}O_{60}$.

Glass (Batch composition)	Composition measured by EDS ($\pm 2\%$)	Density (g/cm^3) ± 0.02 g/cm^3	Molar volume (cm^3/mol) ± 0.09 cm^3/mol	T_g (°C) ± 2 °C
$(1-y)Ge_{23}Sb_7S_{65}Te_5-ySb_{40}O_{60}$				
$Ge_{23}Sb_7S_{65}Te_5$	$Ge_{23}Sb_8S_{64}Te_5$	3.19	16.44	297
$y=0.085$ $Ge_{21}Sb_{10}S_{59}Te_5O_5$	$Ge_{19}Sb_{10}S_{56}Te_4O_{10}$	3.37	15.88	309
$y=0.15$ $Ge_{20}Sb_{12}S_{55}Te_4O_9$	$Ge_{19}Sb_{12}S_{52}Te_4O_{13}$	3.38	15.77	297
$y=0.20$ $Ge_{18}Sb_{14}S_{52}Te_4O_{12}$	$Ge_{18}Sb_{14}S_{50}Te_3O_{15}$	3.48	15.46	276
Corresponding sulfo-telluride glasses				
$Ge_{21}Sb_{10}S_{64}Te_5$		3.31	16.41	285
$Ge_{18}Sb_{14}S_{64}Te_4$		3.40	16.39	265

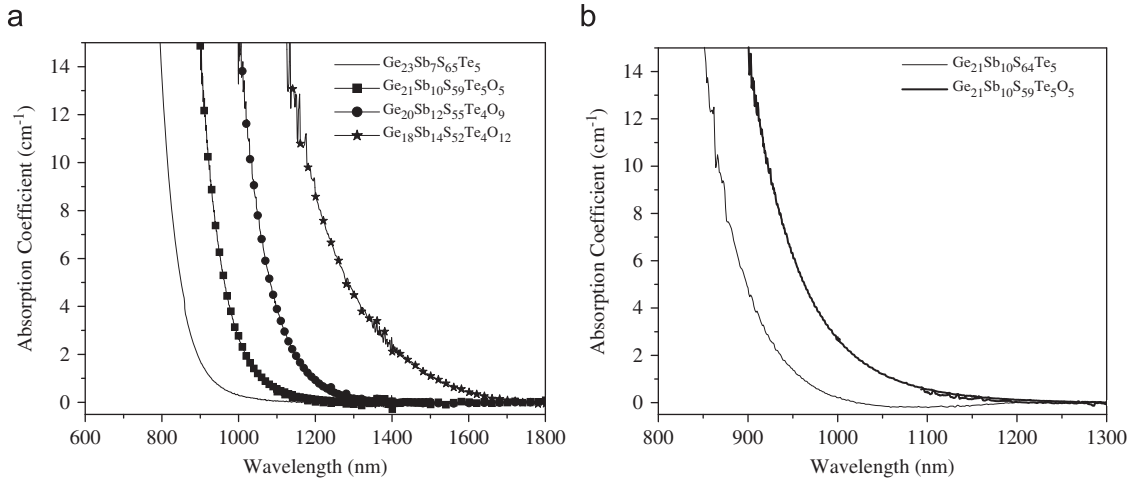

Fig. 4. Absorption spectra of the OChG in the system $(1-y)Ge_{23}Sb_7S_{65}Te_5+ySb_{40}O_{60}$ (a) and of the ChG and OChG with the same ratio between the cations (b).

oxide-containing chalcogenide glass (OChG). As summarized in Table 2, the glass density increases while the molar volume and the T_g decrease when the concentration of Sb_2O_3 increases from $x=0.085$ to 0.20.

As described earlier, both sulfo-telluride glasses and oxy-sulfo-telluride glasses were prepared with the same ratio of cations to allow the separation of the contribution of the S/O ratio change, to that of the Sb-content increase. Since the atomic radii of Ge and Sb are close to each other and the atomic mass of Ge is much smaller than that of Sb atom, changing the composition of the glass by increasing the Sb content at the expense of Ge results in an increase of the density, a decrease of T_g but has no significant effect on the molar volume as seen in Table 2.

For a similar Sb/Ge ratio, the progressive replacement of sulfur with oxygen leads to an increase in the density and the glass transition temperature and a decrease in the molar volume. This again, confirms the incorporation of oxygen into the glass network and the same interpretation as discussed in the previous paragraph.

The absorption spectra of the oxy-sulfo-telluride glasses are exhibited in Fig. 4a and b. It is clearly shown that Sb is not the only contributor to the red shift of the optical band gap but also the replacement of S by O. As explained in the previous paragraph, this may be related to the change in coordination of the Sb between Sb^{3+} and Sb^{5+}. It can be envisioned that partial substitution of oxygen can locally modify the Sb valence state, creating a mixture of valence species in the glass network [21].

The IR absorption spectra of the glasses are shown in Fig. 5. The spectra exhibit the same bands than those seen in Fig. 2, which have been attributed to the presence of S–H, OH and H_2O contamination in the glass network. The same shift to larger wavenumber of the IR absorption edge can be observed in Fig. 5 with an increase of Sb_2O_3 content confirming the incorporation of oxygen in the glass network.

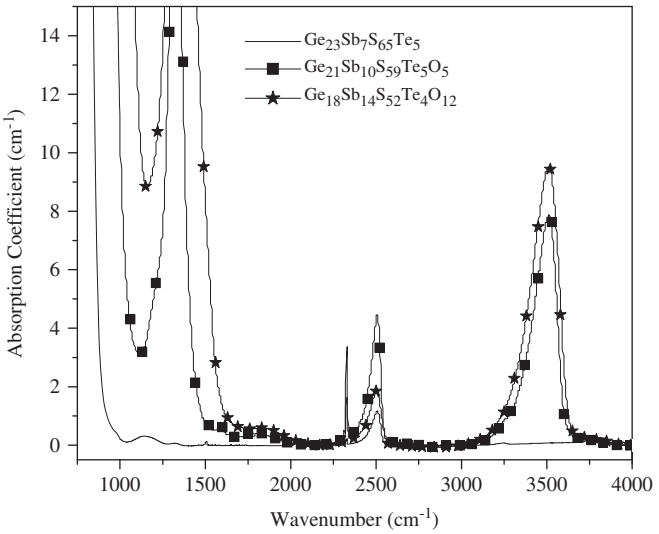

Fig. 5. IR absorption spectra of the OChG in the system $(1-y)Ge_{23}Sb_7S_{65}Te_5+ySb_{40}O_{60}$.

The Raman spectra of the investigated glasses are shown in Fig. 6a, b and c. The spectra exhibit the same bands seen in Fig. 3a and b. With the progressive incorporation of Sb_2O_3 or Sb in the

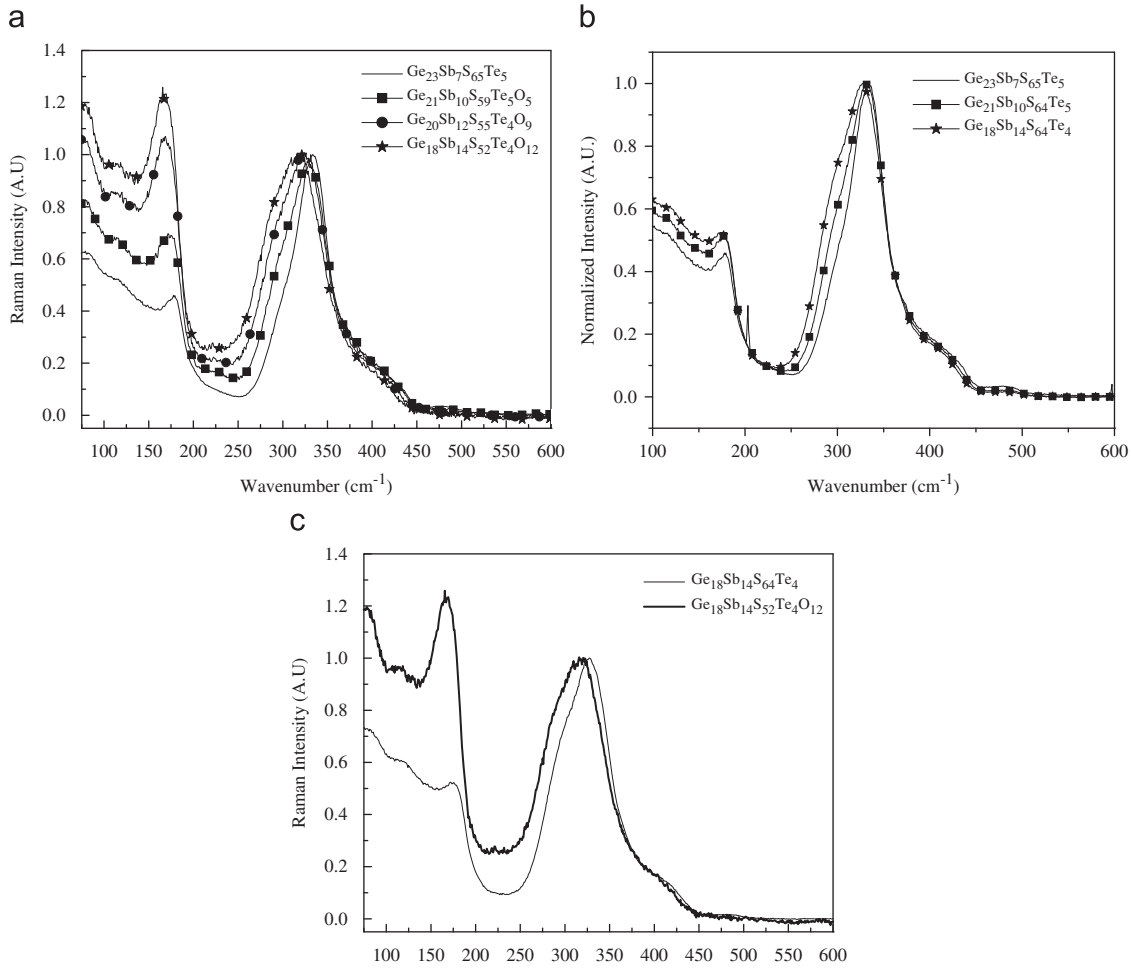

Fig. 6. Raman spectra of the OChG glasses in the system $(1-y)Ge_{23}Sb_7S_{65}Te_5+ySb_{40}O_{60}$ (a), of the sulfo-telluride glasses (b) and of the ChG and OChG with the same ratio between the cations (c).

sulfo-telluride network (Fig. 6a and b), the main band becomes broader and shifts to lower wavenumber, the intensity of the bands in the 450–550 cm^{-1} range decreases and the amplitude of the shoulder at 300 cm^{-1} increases. These variations in the Raman spectra reveal an increase of the SbS_3 units and consequently changes in the interconnectivity of the GeS_4 tetrahedra: a decrease of the $GeS_{4/2}$ units and of the Ge–S–Ge bonds in the glass network when the concentration of Sb_2O_3 or Sb increases.

In Fig. 6c are the Raman spectra of ChG and OChG glasses with the same ratio between the cations. The replacement of sulfur by oxygen leads to an increase in the intensity of the shoulder at ~300 cm^{-1} and of the band at 180 cm^{-1}. The main band also shifts to lower wavenumber. As performed for the previous glass family, the main band was fitted but could not be obtained by simple summation of GeS_2 vibrational features to the oxide spectra. The addition of a new band between 360 and 400 cm^{-1}, different from GeO_4 or GeS_4 tetrahedral sites, and a band at ~320 cm^{-1}, different from SbO_3 and SbS_3 units, were necessary to correctly simulate the spectrum. We observed that the intensity of the band in the 360–400 cm^{-1} range increases with an increase of O content while the amplitude of the band at 320 cm^{-1} increases not only with an increase of O content but also with an increase of Sb content. As explained in the previous paragraph, the band in the 360–400 cm^{-1} range can be attributed to the presence of changes to the formation of edge-sharing $GeS_{4/2}$ tetrahedra (shoulder at ca. 375 cm^{-1}) and/or mixed oxysulfide tetrahedral units GeO_3S, GeO_2S_2 or $GeOS_3$ whereas the contribution at 320 cm^{-1} in the Raman spectra might be related to the formation of species such as SbO_2S or $SbOS_2$ units as suggested in [15].

In summary, the analysis of the IR and Raman spectra shows that introduction of Sb_2O_3 in the sulfo-telluride glass also induces changes in the interconnectivity of GeS_4 tetrahedra due to variations in the S and Sb content, probably leading to the formation of new oxysulfide units such as $GeOS_3$, GeO_2S_2 or GeO_3S and probably SbO_2S or $SbOS_2$ units in glasses. These structural changes are consistent with the increase of the density and T_g and also with the decrease of the molar volume (Table 2).

3.3. Comparison of the physical, thermal, optical and structural properties of OChG prepared using TeO_2 and Sb_2O_3

Oxysulfide glasses with the composition $Ge_{20}Sb_6S_{64}Te_3O_7$ were prepared by melting in vacuum 3 g of the $Ge_{23}Sb_7S_{70}$ glass with TeO_2 and by melting 3 g of the $Ge_{23}Sb_2S_{72}Te_4$ glass with Sb_2O_3 using the same experimental procedure described in the experimental section. The purpose of carrying out this experiment was to evaluate the resulting glass properties as a function of starting material quality. The composition of the two oxysulfide glasses was checked using an energy-dispersive spectroscopy (EDS) system coupled to a scanning electron microscope (SEM).

Table 3
Nominal and analyzed composition, density, molar volume and glass transition temperature (T_g) of the two glasses with the composition $Ge_{20}Sb_6S_{64}Te_3O_7$.

Materials used to process the glass with the composition $Ge_{20}Sb_6S_{64}Te_3O_7$	Density (g/cm^3) ± 0.02 g/cm^3	Molar volume (cm^3/mol) ± 0.09 cm^3/mol	T_g (°C) ± 2 °C
$Ge_{23}Sb_7S_{70}$ glass melted with TeO_2	3.15	15.01	304
$Ge_{23}Sb_2S_{72}Te_4$ glass melted with Sb_2O_3	3.10	15.25	316

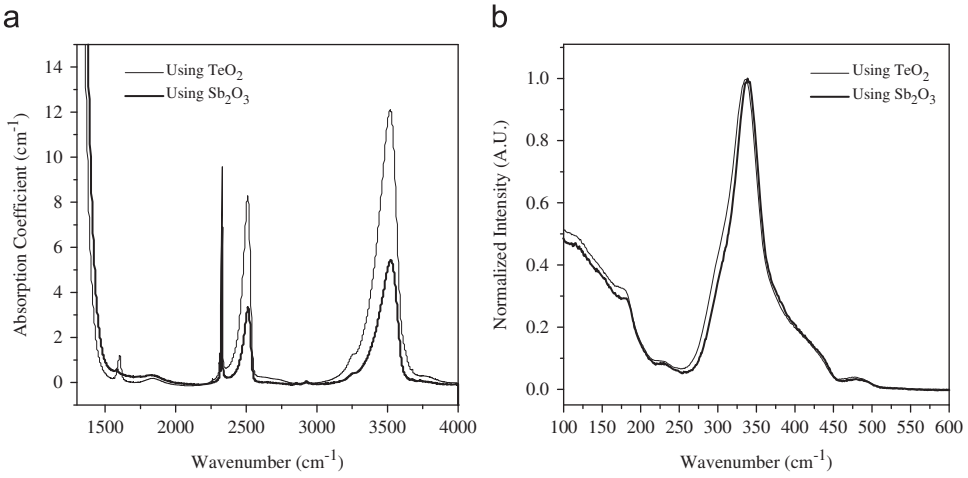

Fig. 7. IR (a) and Raman (b) spectra of two OChG's with the composition $Ge_{20}Sb_6S_{64}Te_3O_7$ prepared using TeO_2 and Sb_2O_3.

The glasses were found to have similar composition within the accuracy of the measurement.

Table 3 lists the density, T_g and molar volume of the two new glasses. One can see that while the new glasses have similar composition, the glasses possess slightly different physical and thermal properties. The oxy-sulfo-telluride glass prepared using TeO_2 has a slightly higher density, lower molar volume and T_g than the glass prepared with Sb_2O_3. As seen in Fig. 7a, the infrared absorption spectra of both glasses exhibit absorption bands related to –S–O–, S–H complexes, molecular H_2S and H_2O. As the intensity of these bands is larger in the spectrum of the glass prepared using TeO_2 as compared to the glass processed with Sb_2O_3, it is possible to think that the tellurium oxide powder is more hygroscopic than the antimony oxide powder. The Raman spectra of the glasses are exhibited in Fig. 7b. The position of the main band of the glass prepared with Sb_2O_3 is slightly shifted to longer wavenumber compared to that of the glass processed with TeO_2, indicating that the glasses with similar composition have slightly different structure as suspected from their different physical, thermal and optical properties probably. This preliminary result shows that the choice of the oxide-based powder might influence the physical, thermal, optical and structural properties of the resulting oxy-sulfo-telluride glass as suggested in [15]. New glasses with different O/S ratio should be processed using TeO_2 and Sb_2O_3 to complement the study and confirm the effect of the oxide-based powder on the physical, thermal, optical and structural properties of the oxy-sulfo-telluride glass.

4. Conclusions

In this paper, we have demonstrated that new oxy-sulfo-telluride glasses can be prepared using a two-melt process using Sb_2O_3 or TeO_2 additions to pre-melted ChG materials. We have shown that an increase of the oxygen content increases the cut-off wavelength probably due to the changes in the Sb coordination, the density and the glass transition temperature and decreases the molar volume of the glass. IR and Raman spectroscopies were useful tools in the study of the structural changes induced by the progressive incorporation of TeO_2 or Sb_2O_3. The compositional dependence of the Raman spectra suggests the formation of mixed Ge- and Sb-based oxysulfide units depending on the Sb content and O/S ratio. Finally, we have shown that (i) it is possible to process the glass with the composition $Ge_{20}Sb_6S_{64}Te_3O_7$ by melting the $Ge_{23}Sb_7S_{70}$ glass with TeO_2 or the $Ge_{23}Sb_2S_{72}Te_4$ glass with Sb_2O_3 and (ii) that the choice of the oxide-based powder might slightly modify the physical, thermal, optical and structural properties of the resulting oxy-sulfo-telluride glass.

Acknowledgments

The authors acknowledge the support of the National Science Foundation, International REU program (#ENG-0649230) whose support of this effort provided international research experiences to the undergraduates (CS) participating in this work. The authors would also like to thank Lockheed Martin Missiles and Fire Control for the summer internship (of JJ), as well as the support of the Sandia NINE program.

References

[1] Z. Ling, H. Ling, Z. Cheng Shan, J. Non-Cryst. Solids 184 (1995) 1.
[2] J. Znobrik, J. Stetzif, I. Kavich, V. Osipenko, I. Zachko, N. Balota, O. Jakivchuk, Ukr. Phys. J. 26 (1981) 212.
[3] I. Kang, T. Krauss, F. Wise, B. Aitken, N. Borrelli, J. Opt. Soc. Am. B 12 (1995) 2053.
[4] L. Zan, L. Huang, C. Zhang, J. Non-Cryst. Solids 184 (1995) 1–4.
[5] H. Nasu, Y. Ibara, K. Kubodera, J. Non-Cryst. Solids 110 (1989) 229–234.
[6] D. Freeman, C. Grillet, M. Lee, C.L.C. Smith, Y. Ruan, A. Rode, M. Krolikowska, S. Tomljenovic-Hanic, C. Martijn de Sterke, M. Steel, B. Luther-Davies, S. Madden, D. Moss, Y. Lee, B. Eggleton, Photonics Nanostruct. 6 (2008) 3–11.
[7] A. Pearson, Mod. Aspects Vit. State 3 (1964) 29.

[8] S. Cherukulappurath, M. Guignard, C. Marchand, F. Smektala, G. Boudebs, Opt. Commun. 242 (2004) 313–331.
[9] T. Cardinal, K.A. Richardson, H. Shim, A. Schulte, R. Beatty, K. Le Foulgoc, C. Meneghini, J.F. Viens, A. Villeneuve, J. Non-Cryst. Solids 256–257 (1999) 353.
[10] S. Santhanam, A.K. Chaudhuri, Bull. Mater. Sci. 3 (1981) 295–299.
[11] J. Quinn, V. Nguyen, J. Sanghera, I. Lloyd, P. Pureza, R. Miklos, I. Aggarwal, J. Non-Cryst. Solids 325 (2003) 150–157.
[12] L. Petit, K. Richardson, B. Campbell, G. Orveillon, T. Cardinal, F. Guillen, C. Labrugere, P. Vinatier, M. Couzi, W. Li, S. Seal, Phys. Chem. Glasses 45 (2004) 315–321.
[13] C. Maurel, T. Cardinal, P. Vinatier, L. Petit, K. Richardson, F. Guillen, M. Lahaye, M. Couzi, F. Adamietz, V. Rodriguez, M. Bellec, L. Canioni, Mat. Res. Bull. 43 (2008) 1179–1187.
[14] C. Maurel, L. Petit, M. Dussauze, E. Kamitsos, M. Couzi, T. Cardinal, A. Miller, H. Jain, K. Richardson, J. Solid State Chem. 181 (2008) 2869–2876.
[15] L. Petit, J. Abel, T. Anderson, J. Choi, V. Nazabal, V. Moizan, M. Couzi, M. Richardson, C. Maurel, T. Cardinal, K. Richardson, J. Solid State Chem. 182 (2009) 2646–2655.
[16] Z.H. Zhou, H. Nasu, T. Hashimoto, K. Kamiya, J. Mater. Res. 14 (1999) 330.
[17] Y. Kim, J. Saienga, S.W. Martin, J. Non-Cryst. Solids 351 (2005) 1973–1979.
[18] N. Terakado, K. Tanaka, J. Non-Cryst. Solids 354 (2008) 1992–1999.
[19] A.N. Sreeram, A.K. Varshneya, D.R. Swiler, J. Non-Cryst. Solids 128 (1991) 294–309.
[20] V. Pamukchieva, A. Szekeres, K. Todorova, M. Fabian, E. Svab, Zs Revay, L. Szentmiklosi, J. Non-Cryst. Solids 355 (2009) 2485–2490.
[21] V. Sudarsan, S.K. Kulshreshtha, J. Non-Cryst. Solids 286 (2001) 99–107.
[22] D. Lezal, J. Zavadil, M. Prochazka, J. Optoelectron. Adv. Mater. 7 (2005) 2281–2291.
[23] T.S. Kavetskyy, A.P. Kovalskiy, V.D. Pamukchieva, O.I. Shpotyuk, Infra. Phys. Technol. 41 (2000) 41–45.
[24] L. Petit, N. Carlie, K. Richardson, Y. Guo, A. Schulte, B. Campbell, B. Ferreira, S. Martin, J. Phys. Chem. Solids 66 (2005) 1788–1794.
[25] G. Lucovsky, F.L. Galeener, R.C. Keezer, R.H. Geils, H.A. Six, Phys. Rev. B 10 (1974) 5134–5146.
[26] K. Murase, T. Fukunaga, Y. Tanaka, K. Yakushiji, I. Yunoki, Physica B 117 & 118 (1983) 962–964.
[27] P. Boolchand, J. Grothaus, M. Tenhover, M.A. Hazle, R.K. Grasselli, Phys. Rev. B 33 (1986) 5421–5434.
[28] E. Kamitsos, J. Kapoutsis, G. Chryssikos, G. Taillades, A. Pradel, M. Ribes, J. Solid State Chem. 112 (1994) 255–261.
[29] K. Andrikopoulos, S. Yannopoulos, A. Kolobov, P. Fons, J. Tominaga, J. Phys. Chem. Solids 68 (2007) 1074–1078.
[30] K. Andrikopoulos, S. Yannopoulos, G. Voyiatzis, A. Kolobov, M. Ribes, J. Tominaga, J. Phys. Condens. Matter 18 (2006) 965.
[31] H. Yoon, W. Jo, E. Cho, S. Yoon, M. Kim, J. Non-Cryst. Solids 352 (2006) 3757–3761.